J Atmos Chem (2010) 65:13–35
DOI 10.1007/s10874-010-9179-5

Downward transport and modification of tropospheric ozone through moist convection

Xiao-Ming Hu · Jose D. Fuentes · Fuqing Zhang

Received: 20 September 2010 / Accepted: 26 November 2010 /
Published online: 24 December 2010

Abstract This study estimated the largely unstudied downward transport and modification of tropospheric ozone associated with tropical moist convection using a coupled meteorology-chemistry model. High-resolution cloud resolving model simulations were conducted for deep moist convection events over West Africa during August 2006 to estimate vertical transport of ozone due to convection. Model simulations realistically reproduced the characteristics of deep convection as revealed by the estimated spatial distribution of temperature, moisture, cloud reflectivity, and vertical profiles of temperature and moisture. Also, results indicated that vertical transport reduced ozone by 50% (50 parts per billion by volume, ppbv) in the upper atmosphere (12–15 km) and enhanced ozone by 39% (10 ppbv) in the lower atmosphere (<2 km). Field observations confirmed model results and indicated that surface ozone levels abruptly increased by 10–30 ppbv in the area impacted by convection due to transport by downdrafts from the upper troposphere. Once in the lower troposphere, the lifetime of ozone decreased due to enhanced dry deposition and chemical sinks. Ozone removal via dry deposition increased by 100% compared to non-convective conditions. The redistribution of tropospheric ozone substantially changed hydroxyl radical formation in the continental tropical boundary layer. Therefore, an important conclusion of this study is that the redistribution of tropospheric ozone, due to deep convection in non-polluted tropical regions, can simultaneously reduce the atmospheric loading of ozone and substantially impact the oxidation capacity of the lower atmosphere via the enhanced formation of hydroxyl radicals.

Keywords Convection · Ozone · Dry deposition · Tropical meteorology · Greenhouse gases

1 Introduction

Deep tropical convection redistributes trace gases in the atmosphere, with the predominant effect of transporting atmospheric boundary layer (ABL) air masses to the upper

X.-M. Hu · J. D. Fuentes (✉) · F. Zhang
Department of Meteorology, Pennsylvania State University, University Park, PA, USA
e-mail: Jdfuentes@psu.edu

troposphere (Chatfield and Crutzen 1984; Ancellet et al. 2009; Dickerson et al. 1987; Thompson et al. 1997; Lelieveld and Crutzen 1994; Lu et al. 2000; Ridley et al. 2004; Pan et al. 2010). Based on carbon monoxide (CO) measurements and satellite-derived deep convective cloud climatology, Thompson et al. (1994) concluded that half of the CO entering the ABL over the central United States is transported upward by deep convection. Bertram et al. (2007) presented a statistical representation of the aggregate effects of deep convection on the chemistry of the upper troposphere based on aircraft observations and estimated that the convective turnover rate of the upper troposphere is between 0.1 and 0.2 day^{-1}. In an idealized numerical modeling study, Mullendore et al. (2005) showed that boundary layer tracers were transported aloft up to the lower stratosphere via convection. Substantial ozone (O_3) formation can occur in the free troposphere following the detrainment of deep convection over an area where ABL is enriched with O_3 precursors such as nitrogen oxides, volatile organic compounds, and CO (Pickering et al. 1992a, b, 1996). In remote environments, where O_3 and its precursors exist in low concentrations, deep convection can transport clean air masses to upper regions of the troposphere (Wang et al. 1995; Pickering et al. 2001). The upward transport can partly explain the nearly O_3-depleted air layers observed in the free troposphere (Kley et al. 1996; Solomon et al. 2005; Takashima et al. 2008). These studies mostly focused on the upward transport of trace gases by deep convection. However, recent field investigations (Betts et al. 2002; Sahu and Lal 2006; Grant et al. 2008a) reported the downward transport of O_3 from the free troposphere to the ABL by tropical convection and concluded that convective storms increase O_3 levels in the ABL by as much as 20 to 30 ppbv.

Using a global three-dimensional (3-D) model, driven by monthly-averaged winds with a resolution of $10° \times 10°$ horizontally and 100 hPa vertically, Lelieveld and Crutzen (1994) concluded that convective processes reduce the tropospheric O_3 loading by 20%. In that study, the mass exchange associated with deep convective was parameterized as a stochastic process based on the frequency of deep convection occurrence. The model employed by Lelieveld and Crtuzen (1994) did not explicitly represent moist convection due to its coarse spatial and temporal resolution. Lawrence et al. (2003) also studied the global impact of vertical transport associated with deep cumulus convection on tropospheric O_3 using a 3-D global model driven by NCEP (National Centers for Environmental Prediction) reanalysis data at the coarse resolution of T21 (spectral transform model until wave number 21, $5.6° \times 5.6°$) with 28 vertical levels up to 2 hPa and a 30-minute time step. The deep convective mixing was parameterized using the method of Zhang and McFarlane (1995). Lawrence et al. (2003) found that enhanced O_3 production due to convective transport of precursors from polluted regions dominated the reduction of O_3 lifetime due to convective mixing over clean regions. In such modeling studies (Lelieveld and Crutzen 1994; Lawrence et al. 2003; Büker et al. 2008), there were limitations in the manner through which the trace gas vertical transport was estimated because deep convection was not explicitly resolved but instead was parameterized in coarse resolution models. Parameterizations of deep convection still remain uncertain (Folkins et al. 2006; Barret et al. 2010; Williams et al. 2010). Therefore, model uncertainties can propagate into the vertical distribution of trace gases if an inappropriate parameterization is employed to estimate the transport of chemical species (Mahowald et al. 1995; Lawrence and Rasch 2005; Donner et al. 2007; Gustafson et al. 2008).

Although previous observations and modeling studies improved the understanding of trace gas transport due to deep moist convection, many processes still remain poorly constrained, including the spatial and temporal extent impacted by convection (Grant et al. 2008a; Salzmann et al. 2008). In this study, 3-D high-resolution cloud-resolving

simulations were carried out for convective storms observed over West Africa to determine whether the downward transport of trace gases can be realistically simulated with mesocale numerical models. Due to deep convection, the enhancement of O_3 in the continental ABL and impacted spatial distribution were determined to estimate changes in O_3 loading resulting from surface deposition rates and chemical reactions. Another objective of this study is to estimate the impacts of enhanced O_3 levels on hydroxyl radical (HO) formation and methane (CH_4) and CO destruction rates in the continental ABL.

2 Methodology

2.1 Research site description

As part of the United States NASA (National Aeronautics and Space Administration) African Monsoon Multidisciplinary Analysis (NAMMA) field campaign, measurements were obtained at a research site (14.66 °N, 17.10 °W) in Kawsara, Senegal during August and September 2006. The research site was located 10 km east of the Atlantic Ocean and 40 km southeast of Dakar, a major urban area in Senegal. Reflectivity data from a Doppler radar and measurements of meteorological variables and chemical species at the research site were collected during the field campaign. The present study focuses on a mesoscale convective storm that approached the research site on August 30–31, 2006 (see DeLonge et al. 2010 for additional details). RF/Chem input is from the MOZART global model output rather than observation. Observations were used to evaluate model results.

2.2 Three-dimensional simulations

To address the research goals, the Weather Research and Forecasting model with Chemistry (WRF/Chem) version 3.2.1 (Grell et al. 2005; Peckham et al. 2009) was used in this study. Three one-way nested domains were employed with grid spacing of 27, 9, and 3 km, respectively (Fig. 1). The first domain covered most of Africa and part of Europe and Asia. The second domain covered part of West Africa, and the third domain

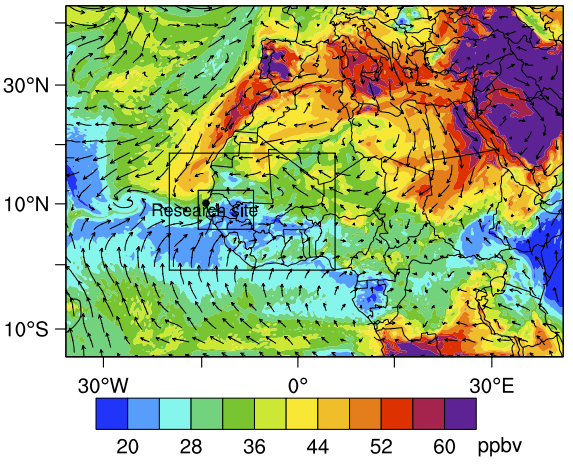

Fig. 1 Simulated surface O_3 mixing ratio at 13:00 UTC on 31 August 2006 using WRF/Chem. Wind vectors show the wind field at 10 m above ground. Two one-way nested domains are marked by the *black boxes*. The inner-most domain has a grid spacing of 3 km, which can spatially resolve individual convective storms

covered Senegal, Gambia, Guinea-Bissau, and parts of Mauritania, Mali, and Guinea (Fig. 1). Each domain had 50 vertical layers extending up to 10 hPa. All model domains used the Dudhia shortwave radiation algorithm (Dudhia 1989), the rapid radiative transfer model (RRTM) (Mlawer et al. 1997) for longwave radiation, the WRF Single-Moment 6-class (WSM6) microphysics scheme (Hong et al. 2004), the Noah land-surface scheme (Chen and Dudhia 2001), and the Yonsei University (YSU) ABL scheme (Hong et al. 2006) with the Monin-Obukhov surface layer method (Monin and Obukhov 1954). The Grell-Dévényi ensemble convective parameterization (Grell and Dévényi 2002) was employed in domains 1 and 2. The convective parameterization was turned off in domain 3 and instead moist convection was explicitly resolved. The NCEP Final (FNL) Global Forecast System (GFS) operational analyses were used for the initial and boundary conditions of all meteorological variables.

To determine gas-phase chemical reactions, the second generation Regional Acid Deposition Model (RADM2) (Stockwell et al. 1990) was used. Anthropogenic emissions of chemical species came from the RETRO (REanalysis of the TROpospheric chemical composition) inventories for the year 2000 (http://retro.enes.org/data_emissions.shtml). The RETRO inventories include the monthly-averaged surface emission for CO, nitrogen oxides, toluene, xylene, benzene, and other non-methane hydrocarbons (NMHC) with a spatial resolution of $0.5° \times 0.5°$. Biogenic emissions were calculated using established algorithms (Guenther et al. 1994). Emissions of nitrogen oxides from lightning and soils were not included in this study. Nitrogen oxides generated from lightning may increase O_3 in upper troposphere by 10–20 ppbv (Sauvage et al. 2007; Aghedo et al. 2007; Saunois et al. 2008). Nitrogen oxides emission from soils peak at the beginning of rainfall season (i.e., June) over the Sahel, which likely contribute to O_3 enhancement over that research region (Jaeglé et al. 2004). On seasonal average, anthropogenic and biogenic emissions play dominant roles in the formation of surface O_3 over Senegal (Aghedo et al. 2007). Initial and boundary conditions for the chemical species were extracted from the output of the global model MOZART4 (Emmons et al. 2010). Simulations were conducted for the period from 12:00 Universal Time Coordinated (UTC, UTC is the same as local time (LT) in Senegal) August 29, 2006 to 00:00 UTC September 1, 2006. The first 36 h of simulation were used as spin-up for the chemical compound fields. Different spin-up times of chemical compound were tested. The variation of O_3 profile was insensitive to the spin-up time since it was dominated by transport under convective conditions. A well-documented mesoscale convective system that moved from West Africa to the Atlantic Ocean on August 30 and 31, 2006 (DeLonge et al. 2010) was investigated. To isolate the effect of moist convection, a sensitivity experiment (hereafter referred to as "NonConvect") was conducted in which latent heating in the model microphysics was turned off. The amplification of deep convection was driven by the release of latent heat through condensation (Houze and Betts 1981). Turning off latent heating in the microphysics scheme suppressed the development of deep convection. Thus, the NonConvect sensitivity simulation was regarded as a reference case without the impact of deep convection. The NonConvect sensitivity simulation is a common practice to investigate the impact of moist convection (e.g., Zhang et al. 2003). Another model sensitivity simulation was carried out but it did not include gas-phase reactions as they were turned off in the modeling domain. The goal was to separate and estimate the contribution of vertical transport versus chemical reactions in the chemical species redistribution. To verify the fidelity of model outputs, reflectivity data from a Doppler radar and measurements of meteorological variables and chemical species at the research site in Senegal were used.

2.3 Zero-dimensional simulations

Enhanced levels of O_3 in the tropical continental ABL can alter regional photochemical processes. To investigate the impacts of enhanced O_3 levels on HO production, and CH_4 and CO destruction rates in the ABL (see R1 and R4), several simulation scenarios were considered. A zero-dimensional model, based on the photochemical mechanism reported by Stockwell (1997), was applied to estimate HO formation and CO and CH_4 destruction rates. Hypothesized scenarios of enhanced O_3 levels ranged from 10 to 70 ppbv and were based on field observations made in the continental tropical ABL (e.g., Grant et al. 2008a; Betts et al. 2002).

$$\begin{array}{lll} \text{R1} & O_3 + h\nu & \rightarrow \quad O_2 + O(^1D) \\ \text{R2} & O(^1D) + H_2O & \rightarrow \quad HO + HO \\ \text{R3} & CH_4 + HO & \rightarrow \quad CH_3 + H_2O \\ \text{R4} & CO + HO & \rightarrow \quad H + CO_2 \end{array}$$

The goal with these calculations was to investigate whether measurably changes in photochemical processes can be expected due to the O_3 downward transport associated with deep convection.

3 Results

A storm approaching the research site in Kawsara, Senegal between 07:00–08:00 UTC on 31 August 2006 was simulated using the 3-km resolution WRF/Chem model (Fig. 2). Model-generated reflectivity values were contrasted with radar reflectivity data, obtained from the NASA dual-polarized, S band Doppler radar, to verify the fidelity of WRF model in simulating the storm (Fig. 2). The approaching time of the simulated storm closely resembled the one observed with the radar. As revealed by radar observations, the storm propagated from the northeast in Senegal to the Atlantic Ocean. However, the simulated storm moved from east to west (Fig. 3). The small discrepancy between model and radar observations likely resulted due to poor model representation of initial conditions of the storm which was derived from the 1°×1° NCEP FNL analysis.

Control model simulations realistically reproduced characteristics of deep convection as revealed by the spatial distribution of temperature at 2 m (T2) and surface water vapor mixing ratio (Fig. 4). The spatial extent of the storm was realistically reproduced by the model. Also, T2 and surface water vapor mixing ratio decreased in regions influenced by deep convection. Decreased temperature near surface in the presence of deep convection was due to evaporative cooling associated with rainfall. Water vapor mixing ratio also decreased in response to the downward transport of drier air masses from the mid-troposphere to the surface.

Surface O_3 mixing ratios increased in the areas directly impacted by the storm. Highest O_3 mixing ratios coincided with storm regions exhibiting maximum reflectivity values (contrast Fig. 5a, b, c with Fig. 3a, b, c). Highest O_3 mixing ratios were associated with leading region of the convective storm where O_3 mixing ratios reached 50–60 ppbv. Results (Fig. 5a, b, c) indicated that storm downdrafts were the principal mechanism to redistribute O_3 from the mid troposphere to the surface. Such vertical transport mechanism is examined in more detailed below.

Simulated vertical cross sections provided details of O_3 distribution and transport associated with deep moist convection (Fig. 6a, b). Boundary-layer air, with low-O_3 content (~30 ppbv), was transported aloft in the updraft region of the storm and detrained between 12 and 14 km above the surface. When the updraft with low-O_3 air mass passed through the

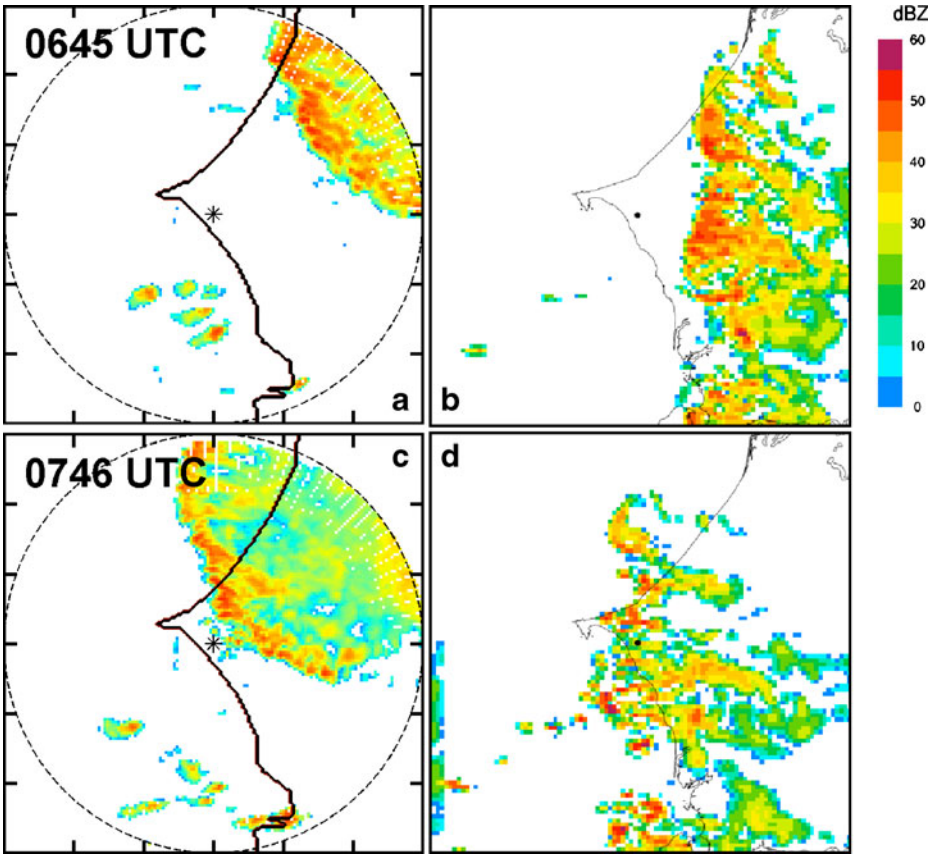

Fig. 2 Radar reflectivity values (r=150 km) at 3 km (in dBZ) from the NASA dual-polarized, S band Doppler radar at **a** 06:45 and **c** 07:46 UTC on 31 August 2006 (data from Delonge et al. 2010) and simulated reflectivity values (in dBZ) at 3 km at **b** 07:00 and **d** 08:00 UTC on 31 August 2006. The research site in Senegal is marked in each panel

middle troposphere, entrainment of O_3-richer air occurred due to the enhanced turbulence mixing provided by buoyancy and shear of the upward-moving air mass. Air mass in the outflow of convection had O_3 levels resembling those found in the lower atmospheric layer (<4 km). This transport of O_3-poor air provided one possible explanation for the observed presence of low-O_3 layers in the upper tropical troposphere (Solomon et al. 2005; Folkins et al. 2006; Kley et al. 1996, 2007; Salzmann et al. 2008; Sauvage et al. 2007; Saunois et al. 2008). Even though the low-O_3 layers were observed over Ocean (e.g., Kley et al. 1996), their driving mechanism is likely the same as illustrated in Fig. 6. Nitric oxide (NO) production due to lightning was proposed to be another reason for the O_3-poor layer in the upper troposphere (Wang and Prinn 2000) as NO can quickly react with O_3 to form nitrogen dioxide (NO_2). However, since lightning production of NO was not included in the model simulation, the estimated upward transport of O_3-poor air by moist convection was a determining factor for the low-O_3 layers simulated in the tropical upper troposphere (Fig. 6). The present study confirms that such low-O_3 layers are most likely associated with the outflow of deep convection. In the present study, the maximum outflow of the investigated convective storm occurred around 14 km above the surface.

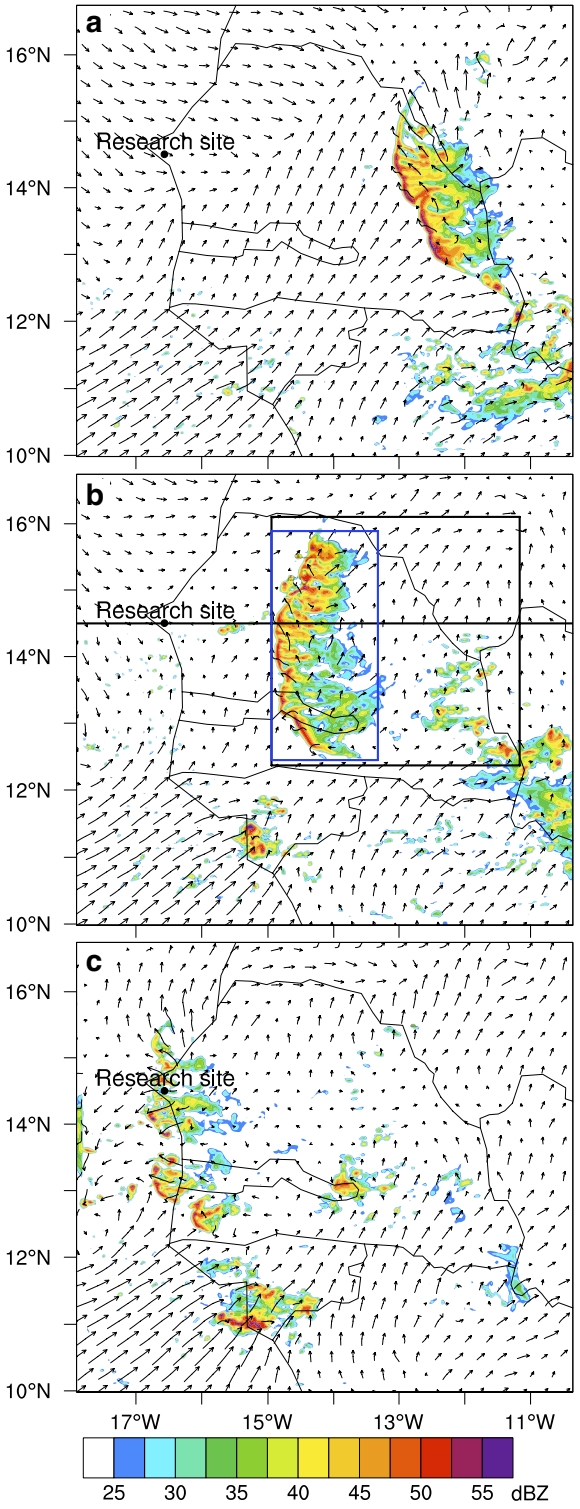

Fig. 3 Simulated cloud maximum reflectivity values in dBZ (**a**, **b**, **c**). The wind vectors show the wind field at 10 m above ground. Model results were obtained for (*top to bottom*) 00:00, 04:00, and 08:00 UTC on August 31, 2006. Black and blue rectangles shown in panel b represent the area included in the calculated vertical mass transport illustrated in Fig. 7. The line through the research site represents the location of cross section shown in Figs. 6 and 8

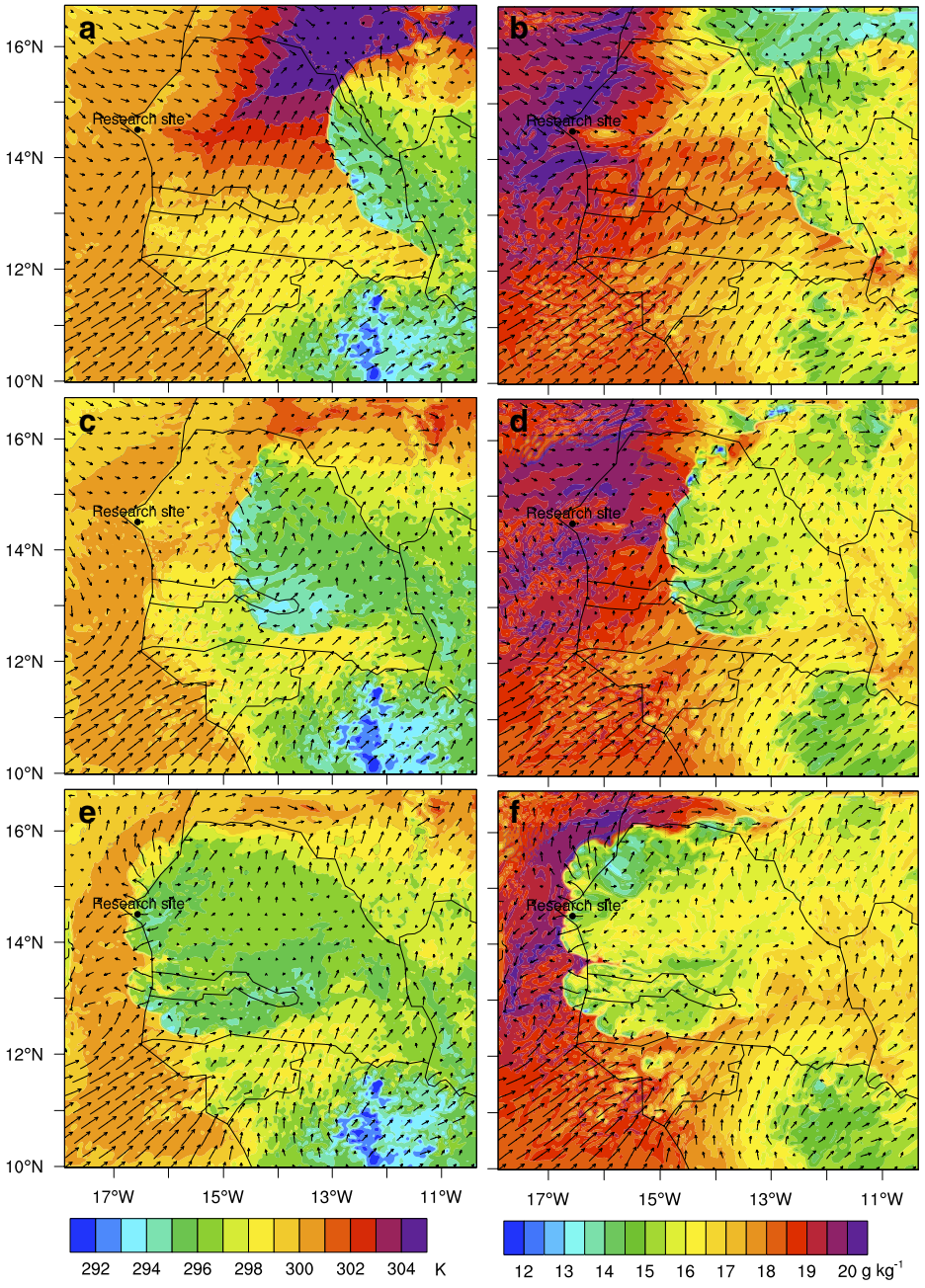

Fig. 4 Simulated spatial distribution of air temperature at 2 m above the surface (T2) in K (**a**, **c**, **e**) and surface specific humidity expressed in g kg^{-1} (**b**, **d**, **f**). Wind vectors show the wind field at 10 m above ground. Model results were obtained for (*top to bottom*) 00:00, 04:00, and 08:00 UTC on August 31, 2006

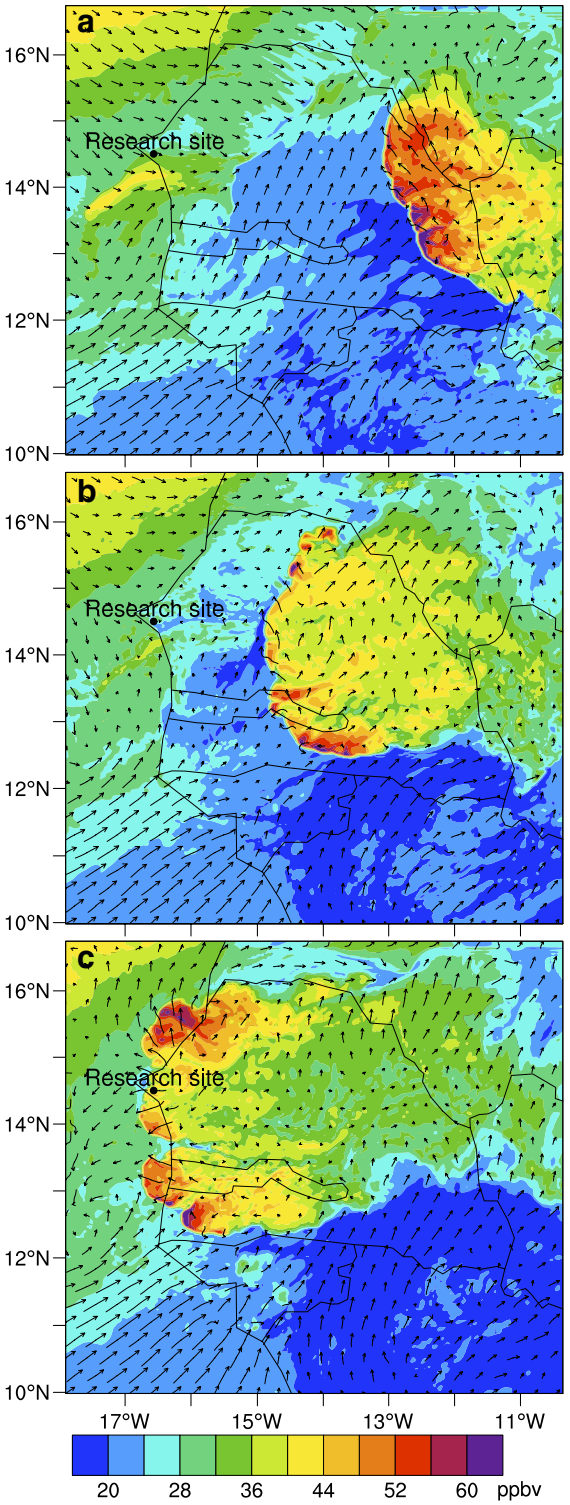

Fig. 5 Simulated spatial distribution of surface O_3 mixing ratio expressed in ppbv. Vectors show the wind field at 10 m above ground. Model results were obtained for (*top to bottom*) 00:00, 04:00, and 08:00 UTC on August 31, 2006

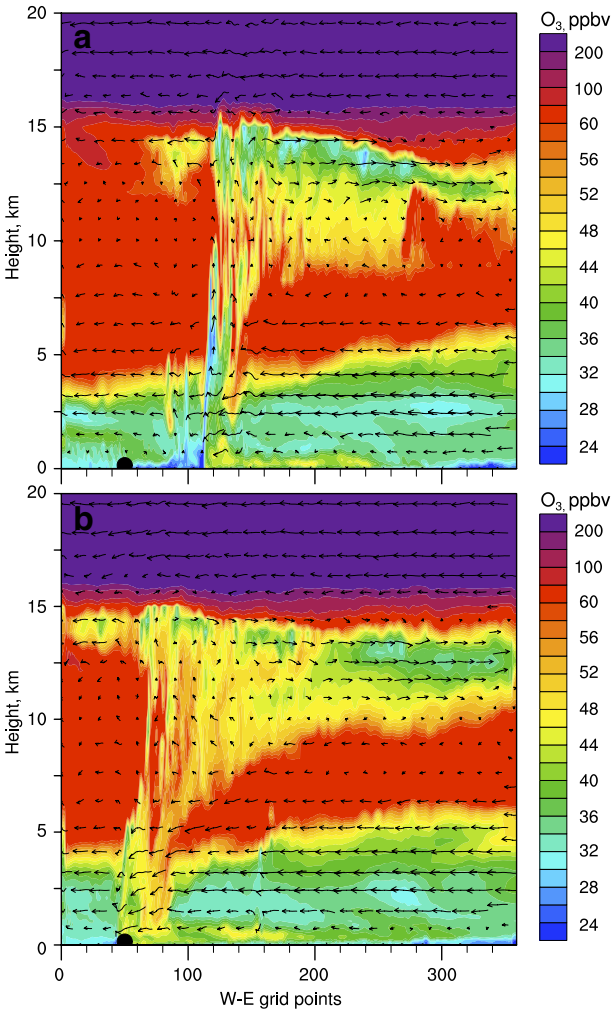

Fig. 6 Ozone vertical distribution for the west-east cross section passing through the research site. Model results were obtained for **a** 04:00 and **b** 08:00 UTC on August 31, 2006. The storm moved from east to west

Within the core of the storm, downdrafts trailed the flank of deep convection and transported the O_3-rich air downward from the upper troposphere to the surface with air entrainment in the middle troposphere. When the storm downdraft reached the surface, the O_3 mixing ratio was nearly 40 ppbv. Vertical mixing of O_3 occurred mostly in the core of the deep convection region whereas horizontal transport dominated in the larger area covered by the stratiform part of the storm (Fig. 6). When integrated and averaged over the core convective region (denoted by the rectangle shown in Fig. 3b), the upward mass fluxes exceeded (by a factor of two around the altitude of 10 km) the downward air mass transport (Fig. 7). The net result of upward and downward transport was the redistribution of tropospheric O_3, increasing (decreasing) its concentrations in the lower (upper) atmosphere. Ozone has different removal rates at different altitude. Therefore, such transport can modify the O_3 tropospheric loading and thus impact the oxidation capacity of the lower atmosphere. Moreover, this transport mechanism has important implications for parameterizing downward transport of O_3 by deep convection for global O_3 budget estimation.

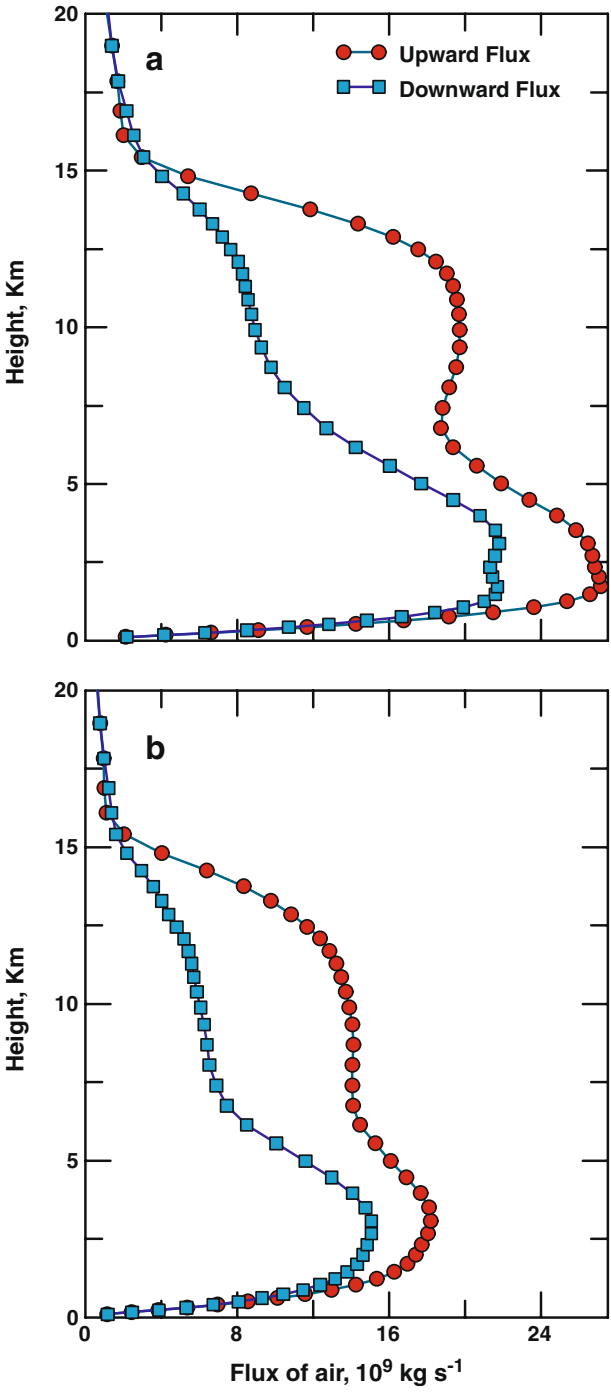

Fig. 7 Modeled mass flux for the regions **a** represented by the *black box* and **b** represented by the *blue box* on Fig. 3b at 04:00 UTC on August 31, 2006. The *blue box* on Fig. 3b includes the convective region with maximum reflectivity larger than 30 dbz, thus panel (**b**) represents the mass flux in the core convective region

Compared with the vertical gradient of O_3, the water vapor mixing ratio was lower in the free troposphere than in the ABL since water vapor came mostly from the evaporation at the surface. As a result, the downdrafts brought dry tropospheric air to the ABL and decreased the surface water vapor mixing ratios (Fig. 4b, d, f).

Compared with O_3, other chemical species such as CO and alkanes have higher mixing ratios near the surface since they are emitted from the ground sources. Thus, their vertical distribution resulting from transport exhibited different patterns compared to that for O_3. For example, in the absence of deep convection, CO was mostly confined in lower atmosphere (Fig. 8). In contrast, in the presence of deep convection, CO was transported to the upper troposphere and detrained at an altitude of 8–15 km above the ground (Fig. 8). Downdrafts behind the flank of deep convection transported CO-poor air downward from the free troposphere to the ABL. In this study the strength of CO source from the surface was weak within the 3-km resolution domain. Therefore, the vertical transport of CO in the present investigation was not as prominent as those reported in other studies (e.g., Dickerson et al. 1987; Pickering et al. 1996) where CO remained as high as 200–300 ppbv in the ABL and as high as 160 ppbv in the convective outflow. In such cases, they observed subsequent enhancement of O_3 formation in the convective outflows due to elevated precursors such as CO and NO. However, in the present study, enhanced O_3 formation was not prominent in the convective outflows. A model sensitivity simulation, which did not include gas-phase reactions, was carried out to separate the influence of transport from chemical reactions. For the O_3 vertical cross section, there were only negligible differences between simulations with and without gas-phase reactions in the anvil outflow region (figure not shown). The insignificant enhancement of O_3 formation in the convective outflows was due to the lower emission of O_3 precursors in the study region (Grant et al. 2008b). These results also indicated that tropospheric O_3 was a quasi-conservative scalar and vertical transport played the dominant role in its redistribution during the convective timescale as reported by previous findings (Scala et al. 1990; Hauf et al. 1995; Kley et al. 1997; 2007; Barth et al. 2007).

Profiles and temporal patterns of equivalent potential temperature (θ_E) and O_3 mixing ratio were measured at the research site in Senegal during the simulated storm (Grant et al. 2008a;

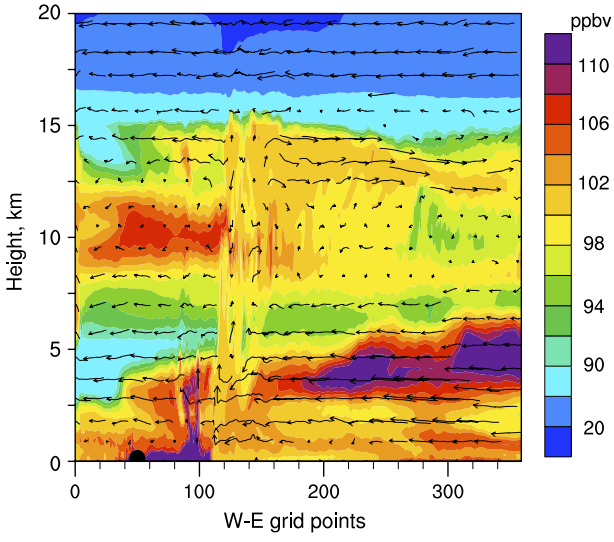

Fig. 8 Vertical distribution of carbon monoxide at 04:00 UTC on August 31, 2006 for the west-east cross section passing through the research site

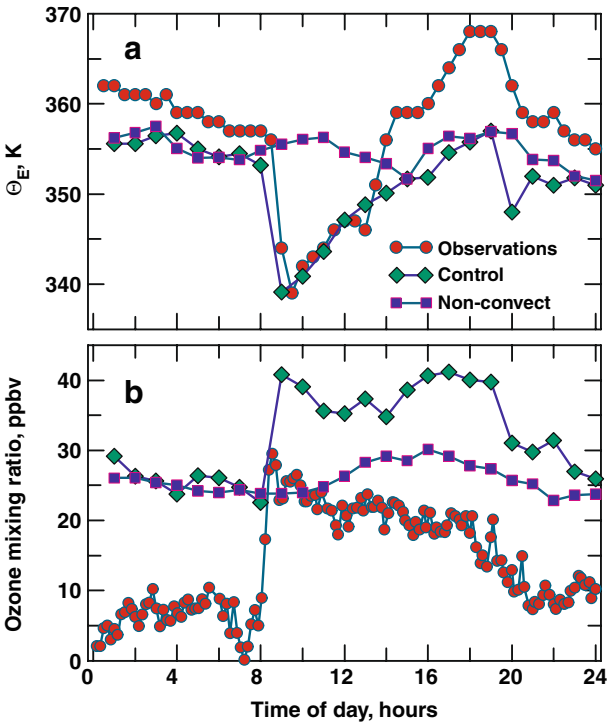

Fig. 9 Observed and simulated **a** surface equivalent potential temperature (θ_E) and **b** O_3 mixing ratio on August 31, 2006 for the research site in Senegal. Model results were obtained from both control and sensitivity (NonConvect) simulations

DeLonge et al. 2010). Observations exhibited abrupt decreases in θ_E and increases in O_3 mixing ratio associated with the passage of the convective storm (Fig. 9). Sharp changes in θ_E and O_3 were reproduced by the control model simulation but not by the sensitivity experiment NonConvect (Fig. 9). Simulated vertical profiles of θ_E and water vapor before and after the passage of the storm are compared with observation (Fig. 10). Comparisons show that the simulation by the WRF/Chem captured the vertical characteristics of the storm; after the passage of the storm, specific humidity and θ_E decreased in the lower atmosphere. In the control simulation, surface O_3 mixing ratio at the research site increased by 18.2 ppbv from 07:00 UTC to 08:00 UTC due to the passage of the storm. This estimated O_3 increase was smaller than the observed O_3 changes which reached ~30 ppbv (Fig. 9b). Simulations verified that the changes in θ_E and O_3 resulted from deep moist convection. Similar abrupt changes in surface θ_E and O_3 mixing ratio were also observed over the Bay of Bengal (Sahu and Lal 2006) and over the Amazon (Betts et al. 2002), which were attributed to convective downdrafts. In the absence of deep convection, O_3 mixing ratios over the research site were overestimated by the control and the NonConvect sensitivity simulations, which likely resulted due to the overestimation of O_3 mixing ratio over the Atlantic Ocean. In general, over the remote oceans, O_3 levels in the ABL are typically less than 10 ppbv (Kley et al. 1996). In contrast, in the present study, simulated O_3 levels over the Atlantic Ocean remained around 20 ppbv. Therefore, O_3 advection from the Atlantic Ocean to the research site contributed to the overestimation of simulated O_3 mixing ratios (Fig. 9b). Over-predicted O_3 levels over the Atlantic Ocean likely resulted due to the inadequacy of the employed chemical mechanism. Over the ocean, where O_3 precursors remain in trace amounts, bromine (Br) is the principal photochemical O_3 sink and can maintain O_3 in the marine ABL at low levels (<10 ppbv) (Vogt et al. 1996; Dickerson et al. 1999; Jacob 2000; Hara et al. 2010). However, bromine

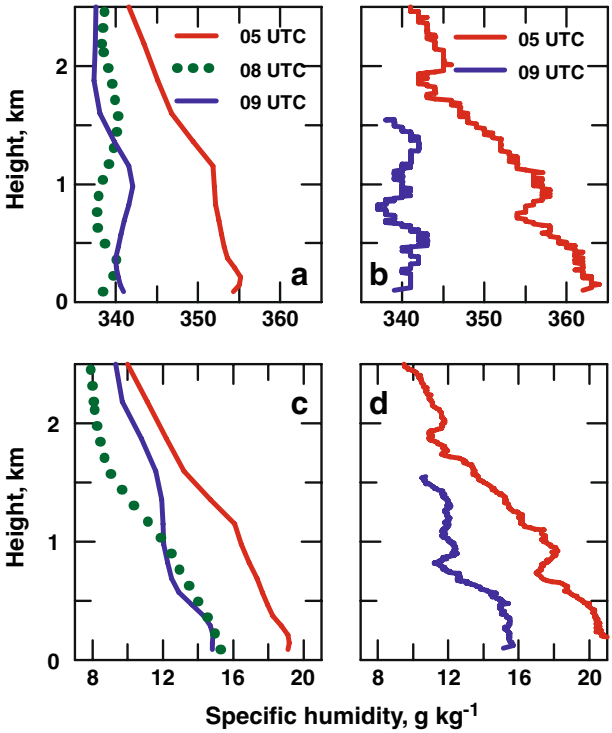

Fig. 10 WRF/Chem simulated vertical profiles of **a** equivalent potential temperature (θ_E) and **c** specific humidity (q) at the research site before and after the passage of the storm and observed vertical profile of **b** θ_E and **d** q (data from DeLonge et al. 2010). The storm approached the research site at 0805 UTC while the model results showed the storm reached the site between 07:00 and 08:00 UTC

sink is not included in the chemical mechanism used in this study and likely contributed to the overestimation of O_3 over the Atlantic Ocean.

Between 3 and 12 km above the ground (below 2.5 km), θ_E was higher (lower) in the control simulation than in the NonConvect experiment over the storm area (Fig. 11a), due to diabatic heating associated with precipitation processes between 3 and 12 km and evaporative cooling in the lower layers (Schumacher et al. 2007). Compared to the NonConvect simulation, O_3 in the lower atmosphere (<2 km) was enhanced by 39% (10 ppbv). In contrast, O_3 in the upper atmosphere (12–15 km) was reduced by 50% (50 ppbv) in response to convective transport which injected low-O_3 ABL air into the upper troposphere and brought O_3-rich upper tropospheric air down to the lower troposphere (Fig. 11b). The O_3 transport associated with convective storms, estimated for the control and the NonConvect simulations, was in good agreement with the conceptual model proposed in Grant et al. (2008a) regarding the dynamics of O_3 redistribution in the troposphere due to deep moist convection. Ozone profiles estimated with the control simulation (Fig. 11b) were consistent with the "S" shaped vertical O_3 profiles, which were typically observed in West Africa (Reeves et al. 2010). Moreover, the present results extend previous findings (Pickering et al. 1992a; b) and indicat that deep convection can efficiently transport primary pollutants (e.g., CO, nitrogen oxides (NO_X), etc.) from the ABL to the free troposphere where enhanced O_3 production can occur in the outflow region of the storm due to the detrainment of O_3 precursors. In the present case, however, the ABL was relatively clean due to minimum anthropogenic gas emissions (e.g., Grant et al. 2008b), and thus O_3 production was negligible in the outflow region of the deep convection.

Dry deposition is an important regional and global sink for O_3 (Jacob and Wofsy 1990; Sigler et al. 2002; Saunois et al. 2009). The O_3 dry deposition velocity (V_d) in the WRF/

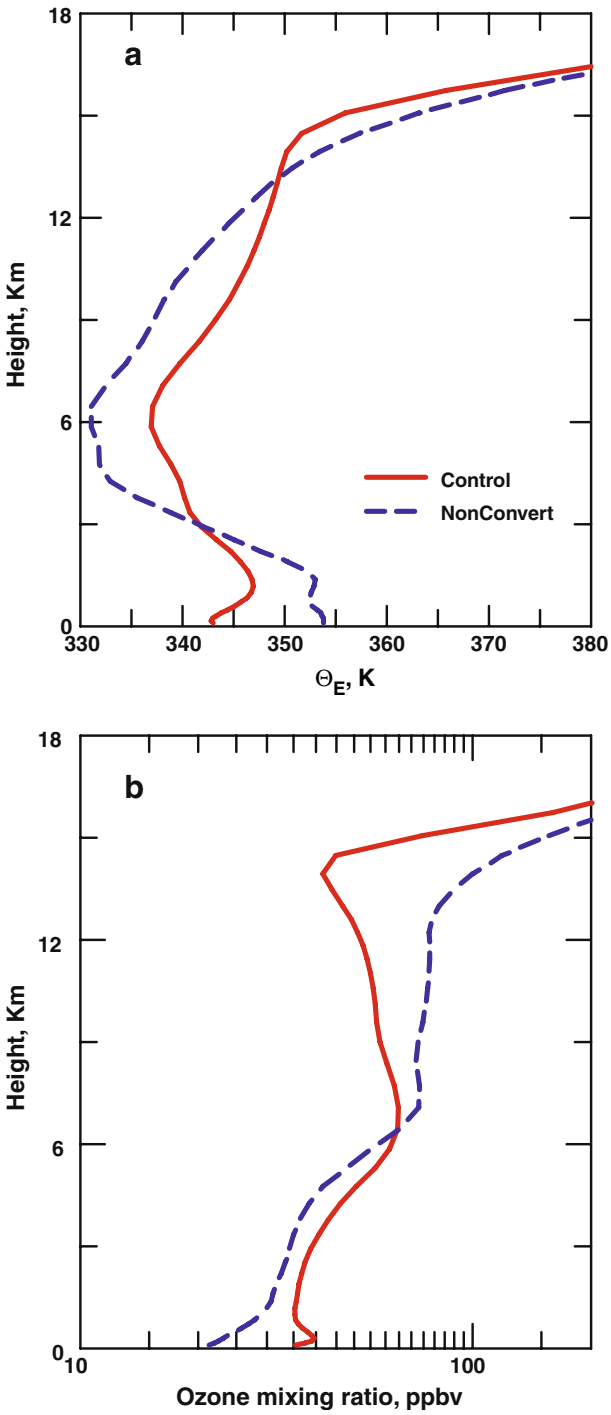

Fig. 11 Mean vertical profile of equivalent potential temperature (θ_E) and O_3 mixing ratio over storm area at 04:00 UTC on August 31, 2006. Model results were obtained from both **a** control and **b** sensitivity (NonConvect) simulations

Chem model was estimated using the method reported by Wesley (1989). The simulated O_3 V_d showed latitudinal gradients in West Africa (figure not shown). To the north of ~10 °N, the O_3 V_d was less than 0.3 cm s^{-1} while V_d was greater than 0.4 cm s^{-1} to the south of 10 °N at 13:00 UTC on 31 August (figure not shown). This result was caused by the transition of land surface from mosaic forest and savanna in the south of ~10 °N to desert in the north. Relatively high O_3 V_d was reported over vegetation (as high as 0.4–1.5 cm s^{-1}) in West Africa (Cros et al. 2000). Latitudinal gradients in O_3 V_d was consistent with the study of Saunois et al. (2009) who estimated that O_3 dry deposition fluxes over vegetation south of 12°N in West Africa were 2–3 times of that north of 12°N. At the research site, on August 31, 2006 diurnal variations in O_3 V_d estimated with WRF/Chem was comparable with V_d estimates obtained using the one-dimensional model of Sigler et al. (2002) reported in Grant et al. (Grant et al. 2008a, b) (figure not shown). The WRF/Chem model estimated maximum O_3 V_d values around 0.75 cm s^{-1} during daytime in response to strong turbulence and biologically active biomass present in Senegal during the rainy season (Grant et al. 2008a). Due to enhanced turbulence, convection also augmented O_3 surface V_d (Fig. 12). In the absence of convection, maximum V_d values reached 0.3–0.4 cm s^{-1} (Fig. 12b). In contrast, in regions dominated by convection maximum V_d values reached 0.5 cm s^{-1} (Fig. 12a). In terms of O_3 fluxes, values as high as 40 μmol m^{-2} hr^{-1} were estimated for the region dominated by the convective storm. Ozone fluxes as low as ~10 μmol m^{-2} hr^{-1} were determined for the same region by the NonConvect simulation (figure not shown). Thus, the O_3 loading was reduced because convection transported O_3 from the free tropospheric to the surface where it could be effectively removed via enhanced dry deposition processes.

During the daytime, photolysis of O_3 and the subsequent reaction of excited atomic oxygen with water vapor was the main HO source (see R1 and R2), but the HO production decreased in the region dominated by deep convection (Fig. 13c) even though the surface O_3 mixing ratio increased (Fig. 13a). This effect resulted from the decreased actinic flux needed for the O_3 photolysis as revealed by reduced short-wave radiation (Fig. 13b) due to the cloud cover associated with deep convection.

Since convective storms with varying degrees of vertical and horizontal scales and propagating velocities can downwardly transport different amounts of O_3 to the surface, several scenarios of enhanced surface O_3 levels (ranging from 10 to 70 ppbv) due to deep convection were investigated using the zero-dimensional model. Simulations with the zero-dimensional model started at 07:00 UTC and continued until midnight. Observed meteorological variables and chemical species (i.e., VOCs and NOx) were used as model input. Seven scenarios were considered, including control (i.e., no changes in O_3 levels), increases in O_3 by 10 ppb, 40 ppb, and 70 ppb at 08:00 UTC without and with clouds. In the scenarios with and without clouds, the solar radiation data obtained at the research site (August 31, 2006 and August 26, 2006) were used as model input. The CO and CH_4 levels were taken for nighttime periods when their mixing ratios attained steady state conditions. The HO radical values were considered to represent maximum rates of formation which took place around 16:00 UTC. Results (Fig. 14) indicate that during cloudless conditions HO mixing ratio changed from 0.19 to 0.37 pptv as O_3 levels increased from 10 to 70 ppbv. During cloudy conditions, even though surface O_3 was enhanced, HO decreased to 0.08–0.14 pptv in response to the attenuation of actinic irradiance. In the case of CO and CH_4, only negligible changes (less than 2 ppbv) were estimated (Fig. 14). In part, the small changes in mixing ratios of CO and CH_4 were the result of their relatively long lifetime with respect to the reaction with HO (28–110 days for CO and 8–12 years for CH_4 in the free troposphere) (Jacobson 2002). These results (Fig. 14) indicate that even small increases

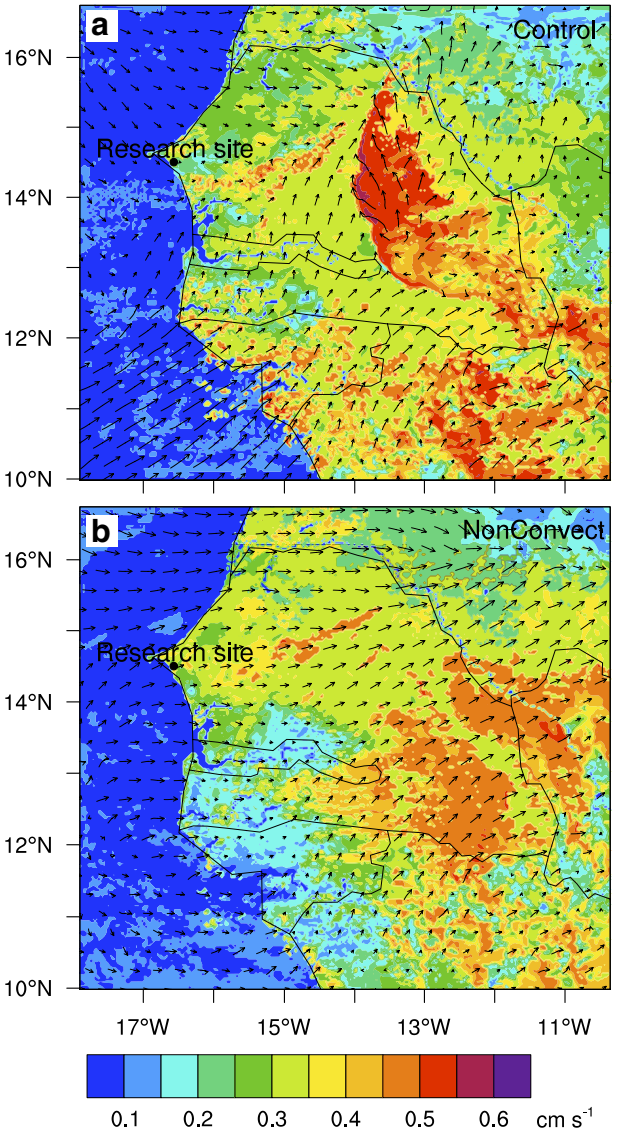

Fig. 12 Ozone dry deposition velocity expressed in cm s^{-1} at 02:00 UTC on August 31, 2006 simulated by **a** the control and **b** the NonConvect sensitivity WRF/Chem simulations

in O_3 in the lower tropical troposphere can augment the HO formation which in turn can change a plethora of chemical cycles, including reactions with hydrocarbon compounds (see R3 and R4).

4 Summary and conclusions

This study demonstrated that existing high-resolution numerical models can realistically represent the principal features associated with initiation and propagation of convective storms in West Africa. Such models can become important tools to investigate processes

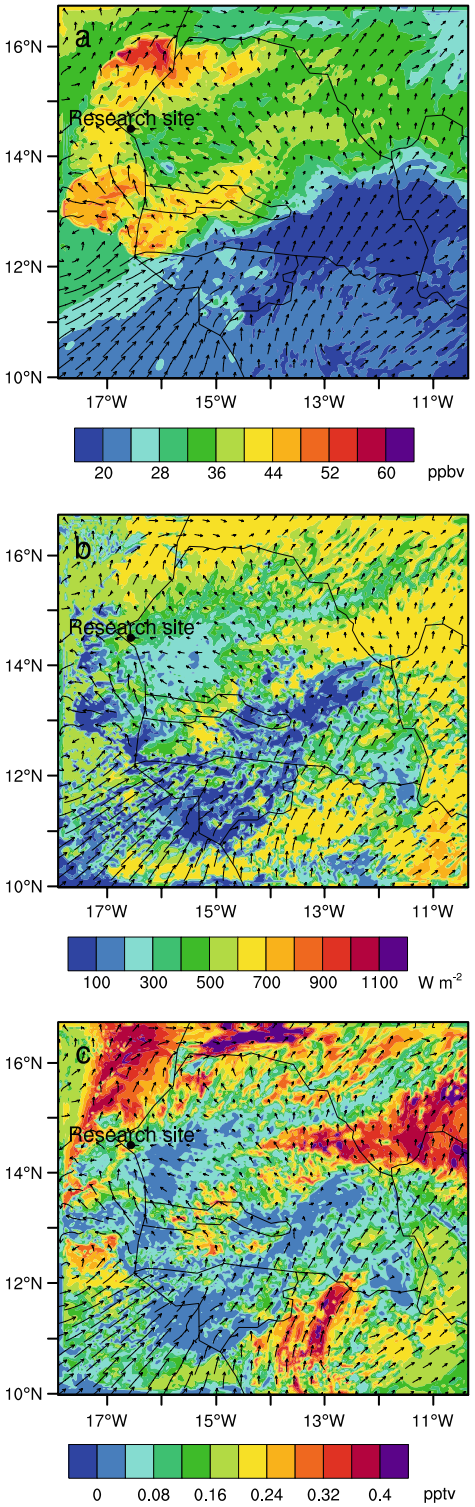

Fig. 13 Simulated spatial distribution of **a** O_3 expressed in ppbv, **b** downward solar radiation given in W m^{-2}, and **d** HO radicals given in pptv at 10:00 UTC on August 31, 2006

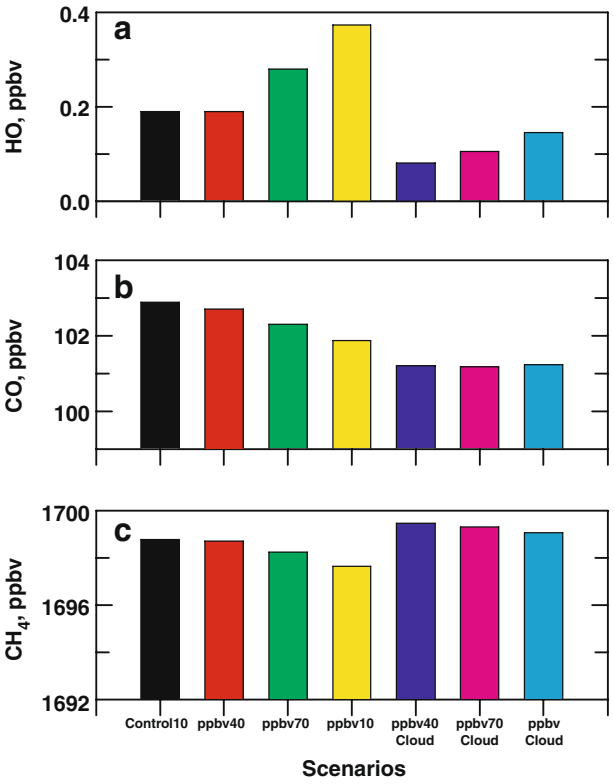

Fig. 14 Changes in mixing ratios of **a** HO, **b** CO and **c** CH_4 near the surface at the research site in Senegal due to enhanced O_3 levels. Simulations with the zero-dimensional model started at 07:00 UTC and continued until midnight. Seven scenarios were considered, including control, increased O_3 in by 10 ppb, 40 ppb, and 70 ppb at 08:00 UTC without and with clouds (see text for additional details)

related to storm dynamics and associated transport and chemistry of reactive chemical species. Therefore, the present study revealed that tropical moist convection effectively redistributes O_3 in the troposphere by transporting nearly-O_3 depleted ABL air to the free troposphere and downwardly moving tropospheric O_3-rich air to the surface. For the storm cases examined in this study, the vertical transport enhanced O_3 by 39% (10 ppbv) in the lower atmosphere (<2 km) and reduced O_3 by 50% (50 ppbv) in the upper atmosphere (12–15 km). Ozone redistribution contributed to a net reduction of tropospheric O_3 loading that resulted due to two concomitant processes. During the rainy season, the reduced O_3 lifetime resulted from the ubiquitous presence of physiologically active vegetation that effectively and permanently removed O_3 from the ABL via dry deposition. The deposition flux increased by as much as 100% due to deep convection compared to non-convective conditions. In addition, photolysis and chemical reactions removed O_3 from the boundary layer. The ensuing photolysis of enhanced O_3 substantially increased HO formation in the continental tropical boundary layer, exceeding 25% compared to non-convective conditions. When taken together, dry deposition and photochemical processes can impact the oxidation capacity of the lower atmosphere, reduce the lifetime of O_3 in the tropical troposphere, and hence decrease the O_3 greenhouse effect. This study mostly focused on the effect of trace gas transport by downdrafts and updrafts associated with convective storms. In the wake of convective storms, atmospheric subsidence could also contribute to the vertical distribution of trace gases. However, the subsidence associated with mesoscale convective storms takes place at larger spatial and time scales (up to several days) which are not considered in the present investigation.

Another important finding of this research concerns the vertical O_3 transport in the core of the deep convection associated with downdrafts and updrafts. When viewed by satellites, storms include both convective and stratiform regions. The present study demonstrated that storm areas dominated by stratiform and anvil regions do not contribute to the vertical O_3 redistribution as much as downdrafts and updrafts. Instead, in the stratiform and anvil regions of storms trace gases are laterally transported away from the core of the deep convection section. Such lateral transport processes can occur at much larger time and spatial scales compared to those dominated by downdrafts and updrafts. Therefore, when attempting to ascertain the trace gas redistribution due to tropical convection employing remote sensing of cloud areas, uncertainties will arise in determining the active region contributing to the vertical transport of gases.

Acknowledgement NASA funded the field research activities associated with NAMMA in Senegal (Grant Number MNX06AC82G). Xiao-Ming Hu received support from the Pennsylvania State University to participate in this research. Kenneth Pratt and David Doughty provided useful comments to improve the original manuscript. Also, two journal reviewers provided excellent comments to improve the original manuscript.

References

Aghedo, A.M., Schultz, M.G., Rast, S.: The influence of African air pollution on regional and global tropospheric ozone. Atmos Chem Phys **7**, 1193–1212 (2007). 10.5194/acp-7-1193-2007

Ancellet, G., Leclair De Bellevue, J., Mari, C., Nedelec, P., Kukui, A., Borbon, A., Perros, P.: Effects of regional-scale and convective transports on tropospheric ozone chemistry revealed by aircraft observations during the wet season of the AMMA campaign. Atmos Chem Phys **9**, 383–411 (2009)

Barret, B., Williams, J.E., Bouarar, I., Yang, X., Josse, B., Law, K., Pham, M., Le Flochmoën, E., Liousse, C., Peuch, V.H., Carver, G.D., Pyle, J.A., Sauvage, B., van Velthoven, P., Schlager, H., Mari, C., Cammas, J.-P.: Impact of West African Monsoon convective transport and lightning NOx production upon the upper tropospheric composition: a multi-model study. Atmos Chem Phys **10**, 5719–5738 (2010). 10.5194/acp-10-5719-2010

Barth, M.C., Kim, S.-W., Skamarock, W.C., Stuart, A.L., Pickering, K.E., Ott, L.E.: Simulations of the redistribution of formaldehyde, formic acid, and peroxides in the 10 July 1996 Stratospheric-Tropospheric Experiment: Radiation, Aerosols, and Ozone deep convection storm. J Geophys Res **112**, D13310 (2007). 10.1029/2006JD008046

Bertram, T. H., et al.: Direct measurements of the convective recycling of the upper Troposphere. Science **315**, doi:10.1126/science.1134548 (2007)

Betts, A.K., Gatti, L.V., Cordova, A.M., Silva Dias, M.A.F., Fuentes, J.D.: Transport of ozone to the surface by convective downdrafts at night. J Geophys Res **107**, 8046 (2002). 10.1029/2000JD000158

Büker, M.L., Hitchman, M.H., Tripoli, G.J., Pierce, R.B., Browell, E.V., Al-Saadi, J.A.: Long-range convective ozone transport during INTEX. J Geophys Res **113**, D14S90 (2008). 10.1029/2007JD009345

Chatfield, R.B., Crutzen, P.J.: Sulfur Dioxide in Remote Oceanic Air: Cloud Transport of Reactive Precursors. J Geophys Res **89**, 7111–7132 (1984)

Chen, F., Dudhia, J.: Coupling an Advanced Land Surface-Hydrology Model with the Penn State-NCAR MM5 Modeling System. Part I: Model Implementation and Sensitivity. Mon Weather Rev **129**, 569–585 (2001)

Cros, B., Delon, C., Affre, C., Marion, T., Druilhet, A., Perros, P.E., Lopez, A.: Sources and sinks of ozone in savanna and forest areas during expresso: Airborne turbulent flux measurements. J Geophys Res **105**, 29347–29358 (2000)

DeLonge, M.S., Fuentes, J.D., Chan, S., Kucera, P.A., Joseph, E., Gaye, A.T., Daouda, B.: Attributes of mesoscale convective systems at the land-ocean transition in Senegal during NASA African Monsoon Multidisciplinary Analyses 2006. J Geophys Res **115**, D10213 (2010). 10.1029/2009JD012518

Dickerson, R.R., et al.: Thunderstorms: An important mechanism in the transport of air pollutants. Science **235**, 460–465 (1987)

Dickerson, R.R., Rhoads, K.P., Carsey, T.P., Oltmans, S.J., Burrows, J.P., Crutzen, P.J.: Ozone in the remote marine boundary layer: A possible role for halogens. J Geophys Res **104**(D17), 21,385–21,395 (1999). 10.1029/1999JD900023

Donner, L.J., Horowitz, L.W., Fiore, A.M., Seman, C.J., Blake, D.R., Blake, N.J.: Transport of radon-222 and methyl iodide by deep convection in the GFDL Global Atmospheric Model AM2. J Geophys Res **112**, D17303 (2007). 10.1029/2006JD007548

Dudhia, J.: Numerical study of convection observed during the winter monsoon experiment using a mesoscale two-dimensional model. J Atmos Sci **46**, 3077–3107 (1989)

Emmons, L.K., et al.: Description and evaluation of the Model for Ozone and Related Chemical Tracers, version 4 (MOZART-4). Geoscientific Model Dev **3**, 43–67 (2010)

Folkins, I., Bernath, P., Boone, C., Donner, L.J., Eldering, A., Lesins, G., Martin, R.V., Sinnhuber, B.-M., Walker, K.: Testing convective parameterizations with tropical measurements of HNO_3, CO, H_2O, and O_3: Implications for the water vapor budget. J Geophys Res **111**, D23304 (2006). 10.1029/2006JD007325

Grant, D.D., Fuentes, J.D., DeLonge, M.S., Chan, S., Joseph, E., Kucera, P., Ndiaye, S.A., Gaye, A.T.: Ozone transport by mesoscale convective storms in western Senegal. Atmos Environ **42**, 7104–7114 (2008a)

Grant, D.D., Fuentes, J.D., Chan, S., Stockwell, W.R., Wang, D., Ndiaye, S.A.: Volatile organic compounds at a rural site in western Senegal. J Atmos Chem **60**, 19–35 (2008b)

Grell, G.A., Dévényi, D.: A generalized approach to parameterizing convection combining ensemble and data assimilation techniques. Geophys Res Lett **29**, 1693 (2002). 10.1029/2002GL015311

Grell, G.A., Peckham, S.E., Schmitz, R., McKeen, S.A., Frost, G., Skamarock, W.C., Eder, B.: Fully coupled "online" chemistry within the WRF model. Atmos Environ **39**, 6957–6975 (2005)

Guenther, A., Zimmerman, P., Wildermuth, M.: Natural volatile organic compound emission rate estimates for U.S. woodland landscapes. Atmos Environ **28**, 1197–1210 (1994)

Gustafson Jr., W.I., Berg, L.K., Easter, R.C., Ghan, S.J.: The Explicit-Cloud Parameterized-Pollutant hybrid approach for aerosol-cloud interactions in multiscale modeling framework models: tracer transport results. Environ Res Lett **3**, 1–7 (2008)

Hara, K., Osada, K., Yabuki, M., Hashida, G., Yamanouchi, T., Hayashi, M., Shiobara, M., Nishita, C., Wada, M.: Haze episodes at Syowa Station, coastal Antarctica: Where did they come from? J Geophys Res **115**, doi:10.1029/2009JD012582 (2010)

Hauf, T., Schulte, P., Alheit, R., Schlager, H.: Rapid vertical trace gas transport by an isolated midlatitude thunderstorm. J Geophys Res **100**, 22,957–22,970 (1995). 10.1029/95JD02324

Hong, S.-Y., Dudhia, J., Chen, S.-H.: A revised approach to ice-microphysical processes for the bulk parameterization of cloud and precipitation. Mon Weather Rev **132**, 103–120 (2004)

Hong, S.-Y., Noh, Y., Dudhia, J.: A new vertical diffusion package with explicit treatment of entrainment processes. Mon Weather Rev **134**, 2318–2341 (2006)

Houze Jr., R.A., Betts, A.K.: Convection in GATE. Rev Geophys Space Phys **19**, 541–576 (1981)

Jacob, D.J., Wofsy, S.C.: Budgets of Reactive Nitrogen, Hydrocarbons, and Ozone Over the Amazon Forest during the Wet Season. J Geophys Res **95**, 16,737–16,754 (1990). 10.1029/JD095iD10p16737

Jacob, D.J.: Heterogeneous chemistry and tropospheric ozone. Atmos Environ **34**, 2131–2159 (2000)

Jacobson, M.Z.: Atmospheric Pollution, History, Science, and Regulation. Cambridge University Press, Cambridge (2002)

Jaeglé, L., Martin, R.V., Chance, K., Steinberger, L., Kurosu, T.P., Jacob, D.J., Modi, A.I., Yoboué, V., Sigha-Nkamdjou, L., Galy-Lacaux, C.: Satellite mapping of rain-induced nitric oxide emissions from soils. J Geophys Res **109**, D21310 (2004). 10.1029/2004JD004787

Kley, D., Crutzen, P.J., Smit, H.G.J., Vomel, H., Oltmans, S.J., Grassl, H., Ramanathan, V.: Observations of near-zero ozone levels over the convective Pacific: Effects on air chemistry. Science **274**, 230–233 (1996)

Kley, D., Smit, H.G.J., Vömel, H., Grassl, H., Ramanathan, V., Crutzen, P.J., Williams, S., Meywerk, J., Oltmans, S.L.: Tropospheric water-vapour and ozone cross-sections in a zonal plane over the central equatorial Pacific Ocean. Q J R Meteorol Soc **123**, 2009–2040 (1997)

Kley, D., Smit, H.G.J., Nawrath, S., Luo, Z., Nedelec, P., Johnson, R.H.: Tropical Atlantic convection as revealed by ozone and relative humidity measurements. J Geophys Res **112**, D23109 (2007). 10.1029/2007JD008599

Lawrence, M.G., von Kuhlmann, R., Salzmann, M., Rasch, P.J.: The balance of effects of deep convective mixing on tropospheric ozone. Geophys Res Lett **30**(18), 1940 (2003). 10.1029/2003GL017644

Lawrence, M.G., Rasch, P.J.: Tracer transport in deep convective updrafts: Plume ensemble versus bulk formulations. J Atmos Sci **62**, 2880–2894 (2005)

Lelieveld, J., Crutzen, P.J.: Role of deep cloud convection in the ozone budget of the troposphere. Science **264**, 1759–1761 (1994)

Lu, R., Lin, C., Turco, R., Arakawa, A.: Cumulus transport of chemical tracers 1. Cloud-resolving model simulations. J Geophys Res **105**, 10,001–10,021 (2000). 10.1029/2000JD900009

Mahowald, N.M., Rasch, P.J., Prinn, R.G.: Cumulus parameterizations in chemical transport models. J Geophys Res **100**, 26,173–26,189 (1995). 10.1029/95JD02606

Mlawer, E.J., Taubman, S.J., Brown, P.D., Iacono, M.J., Clough, S.A.: Radiative transfer for inhomogeneous atmospheres: RRTM, a validated correlated-k model for the longwave. J Geophys Res **102**, 16663–16682 (1997)

Monin, A.S., Obukhov, A.M.: Osnovnye zakonomernosti turbulentnogo peremeshivanija v prizemnom sloe atmosfery (Basic Laws of Turbulent Mixing in the Atmosphere Near the Ground). Tr geofiz inst AN SSSR **24**(151), 163–187 (1954)

Mullendore, G.L., Durran, D.R., Holton, J.R.: Cross-tropopause tracer transport in midlatitude convection. J Geophys Res **110**, D06113 (2005). 10.1029/2004JD005059

Pan, L.L., et al.: The Stratosphere-Troposphere Analyses of Regional Transport 2008 Experiment. Bull Am Meteorol Soc **91**, 327–342 (2010)

Peckham, S. E., et al.: WRF Chem Version 3.1 User's Guide, http://ruc.fsl.noaa.gov/wrf/WG11 (2009)

Pickering, K.E., Thompson, A.M., Scala, J.R., Tao, W.-K., Dickerson, R.R., Simpson, J.: Free Tropospheric Ozone Production Following Entrainment of Urban Plumes Into Deep Convection. J Geophys Res **97**, 17,985–18,000 (1992a)

Pickering, K., Thompson, A., Scala, J., Tao, W., Simpson, J.: Ozone production potential following convective redistribution of biomass burning emissions. J Atmos Chem **14**, 297–313 (1992b)

Pickering, K.E., et al.: Convective transport of biomass burning emissions over Brazil during TRACE A. J Geophys Res **101**, 23,993–24,012 (1996). 10.1029/96JD00346

Pickering, K.E., et al.: Trace gas transport and scavenging in PEM-Tropics B South Pacific Convergence Zone convection. J Geophys Res **106**, 32,591–32,602 (2001). 10.1029/2001JD000328

Reeves, C.E., et al.: Chemical and aerosol characterization of the troposphere over West Africa during the monsoon period as part of AMMA. Atmos Chem Phys **10**, 7575–7601 (2010). 10.5194/acp-10-7575-2010

Ridley, B., et al.: Convective transport of reactive constituents to the tropical and mid-latitude tropopause region: I. Observations. Atmos Environ **38**, 1259–1274 (2004)

Sahu, L.K., Lal, S.: Changes in surface ozone levels due to convective downdrafts over the Bay of Bengal. Geophys Res Lett **33**, L10807 (2006). 10.1029/2006GL025994

Salzmann, M., Lawrence, M.G., Phillips, V.T.J., Donner, L.J.: Cloud system resolving model study of the roles of deep convection for photo-chemistry in the TOGA COARE/CEPEX region. Atmos Chem Phys **8**, 2741–2757 (2008)

Saunois, M., Mari, C., Thouret, V., Cammas, J.P., Peyrillé, P., Lafore, J.P., Sauvage, B., Volz-Thomas, A., Nédélec, P., Pinty, J.P.: An idealized two-dimensional approach to study the impact of the West African monsoon on the meridional gradient of tropospheric ozone. J Geophys Res **113**, D07306 (2008). 10.1029/2007JD008707

Saunois, M., Reeves, C.E., Mari, C.H., Murphy, J.G., Stewart, D.J., Mills, G.P., Oram, D.E., Purvis, R.M.: Factors controlling the distribution of ozone in the West African lower troposphere during the AMMA (African Monsoon Multidisciplinary Analysis) wet season campaign. Atmos Chem Phys **9**, 6135–6155 (2009). 10.5194/acp-9-6135-2009

Sauvage, B., Thouret, V., Cammas, J.-P., Brioude, J., Nédélec, P., Mari, C.: Meridional ozone gradients in the African upper troposphere. Geophys Res Lett **34**, L03817 (2007). 10.1029/2006GL028542

Scala, J.R., et al.: Cloud draft structure and trace gas transport. J Geophys Res **95**, 17,015–17,030 (1990)

Schumacher, C., Zhang, M.H., Ciesielski, P.E.: Heating structures of the TRMM field campaigns. J Atmos Sci **64**, 2593–2610 (2007)

Sigler, J.M., Fuentes, J.D., Heitz, R.C., Garstang, M., Fisch, G.: Ozone dynamics and deposition processes at a deforested site in the Amazon basin. Ambio **3**, 21–28 (2002)

Solomon, S., Thompson, D.W.J., Portmann, R.W., Oltmans, S.J., Thompson, A.M.: On the distribution and variability of ozone in the tropical upper troposphere: Implications for tropical deep convection and chemical-dynamical coupling. Geophys Res Lett **32**, L23813 (2005). 10.1029/2005GL024323

Stockwell, W.R., Middleton, P., Chang, J.S., Tang, X.: The second generation regional acid deposition model chemical mechanism for regional air quality modeling. J Geophys Res **95**, 16,343–16,367 (1990)

Stockwell, W.R., Kirchner, F., Kuhn, M., Seefeld, S.: A new mechanism for regional atmospheric chemistry modeling. J Geophys Res **102**, 25 847–25 879 (1997)

Takashima, H., Shiotani, M., Fujiwara, M., Nishi, N., Hasebe, F.: Ozonesonde observations at Christmas Island (2°N, 157°W) in the equatorial central Pacific. J Geophys Res **113**, D10112 (2008). 10.1029/2007JD009374

Thompson, A.M., Pickering, K.E., Dickerson, R.R., Ellis Jr., W.G., Jacob, D.J., Scala, J.R., Tao, W.-K., McNamara, D.P., Simpson, J.: Convective transport over the central United States and its role in regional CO and ozone budgets. J Geophys Res **99**, 18,703–18,711 (1994)

Thompson, A.M., Tao, W.-K., Pickering, K.E., Scala, J.R., Simpson, J.: Tropical deep convection and ozone formation. Bull Am Meteorol Soc **78**, 1043–1054 (1997)

Vogt, R., Crutzen, P.J., Sander, R.: A mechanism for halogen release from sea-salt aerosol in the remote marine boundary layer. Nature **383**, 327–330 (1996)

Wang, C., Crutzen, P.J., Ramanathan, V., Williams, S.F.: The role of a deep convective storm over the tropical Pacific Ocean in the redistribution of atmospheric chemical species. J Geophys Res **100**, 11,509–11,516 (1995). 10.1029/95JD01173

Wang, C., Prinn, R.G.: On the roles of deep convective clouds in tropospheric chemistry. J Geophys Res **105**, 22,269–22,297 (2000). 10.1029/2000JD900263

Wesley, M.L.: Parameterization of surface resistance to gaseous dry deposition in regional numerical models. Atmos Environ **16**, 1293–1304 (1989)

Williams, J.E., et al.: Global chemistry simulations in the AMMA multimodel intercomparison Project. Bull Am Meteorol Soc **91**, 611–624 (2010). 10.1175/2009BAMS2818.1

Zhang, G.J., McFarlane, N.A.: Sensitivity of climate simulations to the parameterization of cumulus convection in the Canadian Climate Centre general circulation model. Atmos Ocean **33**, 407–446 (1995)

Zhang, F., Snyder, C., Rotunno, R.: Effects of moist convection on mesoscale predictability. J Atmos Sci **60**, 1173–1185 (2003)